

METAL FOAMS FOR ELECTROMAGNETICS: EXPERIMENTAL, NUMERICAL AND ANALYTICAL CHARACTERIZATION

L. Catarinucci*, G. Monti, and L. Tarricone

Innovation Engineering Department, University of Salento, Via per Monteroni, Lecce 73100, Italy

Abstract—This work focuses on the use of metal foams, a relatively new class of materials, for high added-value electromagnetic (EM) shields. First, the Shielding Effectiveness (SE) of aluminum foam slabs is experimentally evaluated, showing very good shielding properties. Successively, accurate numerical models of metal foams are proposed and used in a proprietary Variable-Mesh Parallel Finite Difference Time Domain code, in order to characterize the EM properties of slabs of such materials. Afterwards, a third approach is adopted. It consists in the application of the effective medium theories in order to obtain an analytical EM model of the metal foams; this way, their SE can be evaluated with a negligible computational time by using common mathematical tools. Finally, a methodology to design/analyze customized metal foams for EM shield applications is suggested. It takes advantage from the joint use of the numerical and analytical presented approaches, thus allowing a computationally efficient evaluation of SE and other electromagnetic properties of metal foams. Results demonstrate the suitability of metal foam structures for effective EM shielding in many industrial applications, as well as the accuracy of the proposed analytical and numerical approaches.

1. INTRODUCTION

Metal foams represent a relatively new class of materials which opens new challenging perspectives in many industrial applications. In fact, metal foams are heterogeneous cellular structures made of metal and gas (usually air) characterized by a very low apparent density [1–11]. This gives foams high stiffness-to-weight ratio and lightweight.

Received 29 August 2012, Accepted 12 October 2012, Scheduled 16 October 2012

* Corresponding author: Luca Catarinucci (luca.catarinucci@unisalento.it).

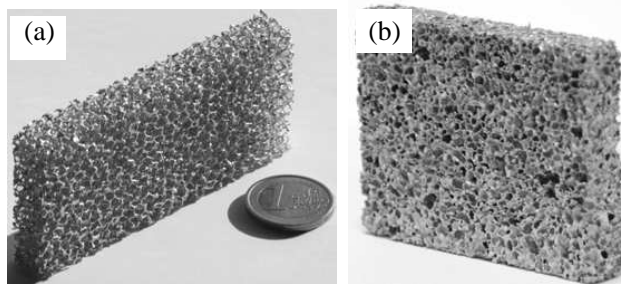


Figure 1. (a) Examples of open-cell and (b) closed-cell aluminum foams; the apparent density is respectively 8% and 6%.

Moreover, their porous structure confers them energy and sound absorption properties, along with thermal insulation and vibration damping capabilities. In Fig. 1 two aluminum foam slabs are shown. The sample of Fig. 1(a) is a Duocel® open-cell foam produced by ERG Aerospace with an apparent density of almost 8%. The structure of this foam allows both light and air to pass through; this particular characteristic can be useful in several applications. Fig. 1(b), instead, is referred to a sample of closed-cell foam with an apparent density of 6%.

It is worth observing that metal foams with different specific physical properties can be produced on demand, varying cell topology (open or closed cells), material (aluminum, copper, titanium etc.), apparent density, and pore size. In such a way, the most appropriate foams can be tailored to specific engineering design applications, ranging from mechanical to automotive, gas and fluid filtration, thermal management and many others [1–10].

One of the possible application areas which has not been deeply investigated so far is electromagnetic compatibility, where the cellular structure of the foams promises good electromagnetic (EM) shielding effectiveness (SE). Moreover, the mechanical properties of the metal foams could represent a real advantage even in this specific domain. In literature, strong effort has been dedicated to the SE evaluation of complex EM screens, including metamaterial-based structures such as regular 3D-wire meshes [12] and arrays of resonant particles [13]. Vice versa, only a previous work of the same authors [14, 15] deals with metal foams EM shields, where an SE analytical investigation has been performed by approximating the open cell metal foam with a 3D-wire array. It is worth noting that, despite the promising results discussed in [14–16], such an approximation implies that the potential effects due to the non-regular and random structure of the foam are not taken into account. To this regard, EM shields realized by using

aluminum foam slabs could have a true added value. Let's consider first magnetic resonance apparatus: the structure of the open-cell foam slabs has the advantage to let air and light pass through, thus reducing claustrophobic discomfort. The same kind of aluminum foams could be attractive for the realization of air-vents in EM shielded environments and also in industrial microwave ovens, where the need to reduce humidity could be easily satisfied. Furthermore, the high vibration damping capabilities and sound absorption properties of closed-cell foams become interesting for the EM shielding of engines.

The evident opportunities of application of these materials in Electromagnetics make their rigorous EM characterization a must [11]. Accordingly, in this work, the analysis of the shielding properties of different kinds of Duocel® aluminum foam slabs has been firstly performed through experimental measurements by varying porosity and apparent density. The obtained interesting shielding capabilities encourage the development of ad-hoc simulation tools for design/analysis purposes.

From a numerical point of view, the EM problem of the rigorous evaluation of the SE metal foams is a challenging task; metal foams have a complex structure, strongly inhomogeneous, thus requiring sophisticated numerical models. The first proposed solution is based on the generation of accurate Finite Difference Time Domain (FDTD)-compatible numerical models, and on their use in a proprietary parallel Variable Mesh (VM) FDTD algorithm [17–24]. In this way, the huge computational requirement due to the intrinsic different length-scales in the simulation domain (for instance, fractions of millimeters for the foam ligaments and tens of centimeters for the antenna-foam distance), can be satisfied. Nevertheless, despite of the advantages in terms of accuracy given by the full-wave tool, the computational time is in some cases excessive and the hardware cost not negligible.

In order to overcome these shortcomings, a simplified and effective analytical EM model of metal foams has been developed by carrying on an effective medium approach. Differently from the fully-analytical approach presented in [14–16], in this work the 3D-wire mesh approximation is not applied anymore and the peculiarities of the foam structure are taken into account by feeding the model through the full-wave simulation of a small numerical foam sample. For the estimation of metal foam SE, the proposed strategy can be directly implemented in common mathematical tools and executed with a negligible computational time. Moreover, such a model is also useful for general EM design and analysis purposes. In fact, if combined with a conventional full-wave simulator, it guarantees adequate accuracy with an affordable computational effort.

2. METAL FOAMS

Although the use of metal foams in innovative mechanical and thermal applications has been steadily increasing over the past decade, foams are quite unfamiliar to other engineering sectors. Nevertheless, the previously mentioned perspective of application in the EM area encourages a detailed EM characterization, taking into account relevant issues such as the metal type, the cell topology (closed or open), the apparent density and the cell size. More specifically, apparent density represents the weight per unit volume of a material, including voids existing in the material itself. It influences foam stiffness, strength, and both electrical and thermal conductivity. As for the pore size, it represents the pore dimension and it is the parameter which mostly affects properties such as optical capacity and fluid flow resistance. The number of pores for linear inches (PPI) is also a parameter used to characterize the foam. Such physical characteristics are intrinsically dependent on the foam manufacturing process and it is worth highlighting that they are strongly related to each other.

Without loss of generality, the foam deeply studied in this paper, potentially very attractive for EM applications, is the one produced by ERG Aerospace and named Duocel® foam. This material consists of small ligaments that are continuously connected in an open-celled foam structure (see Fig. 1(a)). The cells of Duocel® foams are generally 12 or 14-sided polyhedral whose pentagonal or hexagonal faces are formed by five or six ligaments. The open window in each of these faces defines the pore diameter which usually varies from 5 to 100 PPI. As reported in [1], the manufacturing technology is quite sophisticated and it is substantially based on the realization of a preliminary open-cell polymer foam mould template with the desired cell size and apparent density. The polymer is then coated with a mould casting slurry which is then dried and embedded in casting sand. The mould is then baked in order to harden the casting material as well as to decompose and evaporate the polymer template, thus giving a negative image of the foam. This mould is subsequently filled with a metal alloy and cooled, so that a metal with an equivalent shape of the original polymer foam is obtained.

By realizing appropriate foams with specific values of PPI (and consequently of pore sizes) and apparent density, it is possible to obtain a combination of properties considered attractive from an EM point of view.

3. EM SIMULATION TOOLS FOR METAL FOAMS

As already stated, in order to electromagnetically characterize the metal foam structures, a full wave simulator based on the very versatile FDTD algorithm, can be used. Nevertheless, in order to describe the complex foams structure accurately, space step of fractions of millimeters must be used, thus requiring huge computational efforts. Fine space steps, in fact, cause the FDTD time step reduction as well as the excessive growing of the simulation domain size. In the following subsections, a proprietary parallel VM-FDTD algorithm, capable to deal with non uniform meshes in parallel environment, will be briefly illustrated. Moreover, a realistic and very accurate numerical model of metal foams will be realized and presented.

Despite of the achieved accuracy, a less computational intensive approach is necessary in order to allow the adoption of traditional computing platforms. Therefore, an analytical model is also proposed.

3.1. Parallel VM-FDTD

When using uniform FDTD, the characterization of simulated objects with an adequate space resolution obliges the use of such a resolution over the entire simulation domain. This leads to the adoption of a space discretization step larger than the one needed in several parts of the simulation domain. Such an observation is the basis of VM-FDTD algorithms [17–23], which, allowing the existence of different discretization steps in different regions, give a good level of accuracy for the solution using less memory and computational power than the ones needed to obtain the same accuracy with a classical (uniform) FDTD scheme. Moreover, when such a scheme is implemented in a parallel platform, further advantages in terms of computational time are achieved. In fact, differently from standard subgridding techniques, the variable mesh scheme is a natural extension of the parallel FDTD implementation. In VM-FDTD the discretization is performed in a way that each grid cell has only one adjacent grid cell for each one of its six faces. Furthermore, along each direction the space step can be arbitrarily varied, within the limits imposed by the stability criterion, allowing very smooth transitions between a fine and a coarse mesh region. For such reasons, the parallel implementation is based on the same principles of the parallel uniform FDTD, i.e., it adopts the same partition of the simulation domain, based on a balancing of the computation among the different processors, and implements the same communication pattern between adjacent processors.

In order to take into account the different cell-size, three auxiliary vectors can be used, containing the dimension of each cell along x , y

and z . Because of the component location in Yee's cell [23], such values can be directly used wherever E -field space derivatives are evaluated; on the contrary, when H -field space derivatives are considered, the averaged dimension between two adjacent cells must be used. The same kind of arrangement must be applied when computing the absorbing boundary condition as well [23, 24].

3.2. Metal Foams Numerical Models

An FDTD-compatible numerical model of metal foams has been developed, consisting in a binary file that associates the generic space coordinate to the related kind of material (air or aluminum alloy in most cases). In order to accurately reproduce in the FDTD simulation domain the complex and non-regular geometry of metal foams, appropriate algorithms have been developed. Such algorithms emulate the actual metal foam realization procedure described in the previous section. Using this approach, both open and closed-cell numerical models of metal foams can be generated with arbitrary porosity and apparent density. More specifically, the implemented algorithms are based on the generation, in a certain number of random points, of pores of a desired shape (which can be a sphere, but also an open polyhedral when Duocel® foams are modeled): cell size and windows apertures are randomly varied in specified ranges and the intersections between the pores are accurately treated. The final result is a file in the so-called voxel format, where each voxel is a cube, individuated by three Cartesian coordinates, which contains information about the material in that voxel (aluminum or air in the addressed case).

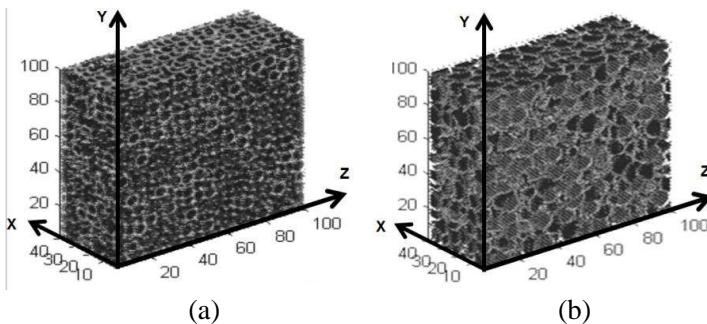


Figure 2. 3D representation of the voxel-files representative of the numerical model of (a) an open-cell and (b) a closed-cell aluminum foam. The axis labels refer to the Cartesian coordinates of each voxel.

In Fig. 2, for instance, the numerical models of two metal foam slabs are reported through the 3D representation of the cubical voxels (whose side is 1 mm) discretizing the foams. The models of Fig. 2 are related to slabs of metal foams of $10 \times 10 \times 4 \text{ cm}^3$. More specifically, the model of Fig. 2(a) represents a case of Duocel® open-cell structure, whilst a case of closed-cell structure is sketched in Fig. 2(b). It can be clearly observed the similarity with the real samples of Fig. 1.

3.3. Metal Foams Analytical Model: An Effective Medium Approach

It is well known that an artificial structure, consisting for example of metallic inclusions in a dielectric host material [25, 26] or of a periodically loaded transmission line [27–35], can be considered as an homogeneous medium at frequencies corresponding to wavelengths much longer than the intrinsic length-scales of the composite (effective medium approach) [25, 26, 36–40]. Indeed, at these frequencies, diffraction phenomena can be neglected and the structure can be described through averaged parameters (effective parameters) derived from the geometrical and electromagnetic properties of its constituents.

The basic idea is to replace the composite under test with a homogeneous medium whose parameters must be set so that the two structures exhibit the same microscopic behaviour. It follows that, with respect to a microscopic point of view, this method implies negligible computational efforts.

According to these observations, an EM effective medium model of metal foams has been investigated. A viable approach is the adoption of the same dispersion model of metals, i.e., the so called Drude model [41, 42]. According to this model, metals are considered to be a gas of electrons freely moving around positive ions. As a consequence, due to this plasma approximation, the model assumes the following expressions for the relative electric permittivity (ε_r) and the relative magnetic permeability (μ_r) of the medium:

$$\varepsilon_r = \left(1 - \frac{\omega_p^2}{\omega^2 - j\gamma\omega} \right), \quad \mu_r = 1; \quad \left(\omega_p^2 = \frac{Ne^2}{m_e} \right). \quad (1)$$

where ω_p [rad/s], N and m_e [eV(m/s)²] are respectively the plasma angular frequency, the electron density and the electron mass. The medium loss is determined by the damping factor γ which is the electron collision rate.

From (1) it is evident that, for frequencies below ω_p , the relative permittivity ε_r assumes negative values resulting in an imaginary wave vector. As a consequence, at these frequencies, metals support only

evanescent modes. For common metals, typical values of ω_p are in the THz range.

In the last years, a large number of studies have demonstrated that the frequency dependence given in (1) can be assumed to model the effective electric permittivity of artificial structures consisting of a metallic wire mesh [43–48]. Specifically, it has been experimentally verified that an array of thin wires behaves like the metal which constitutes the wires, but with a lower plasma frequency [43–48].

These considerations can be extended to metal foams. In fact, with reference to the electron motion constraints, as evident from Fig. 3, the 3D-wire array and a generic metal foam are very similar structures. In both cases only a fraction of the space is filled with metal, thus limiting electron movements. More specifically, it has been demonstrated that a 3D-wire array behaves like a metal with a plasma frequency which depends on the lattice period ‘ a ’ (see Fig. 3) and

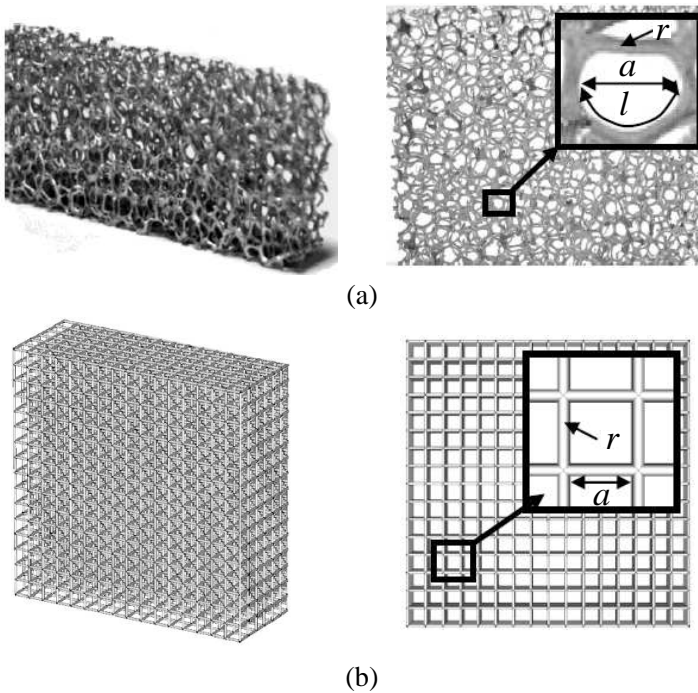


Figure 3. Comparison between (a) a Duocel® open-cell aluminum foam (porosity: 20 PPI, apparent density: 8%) and (b) a 3D metallic wire mesh: perspective view on the left and frontal view on the right. In both cases the insert in the frontal view illustrates the unit cell.

on the wire radius (r) [49]. According to these considerations, metal foams can be modeled like a metal with a plasma frequency depending on their apparent density which, referring to Fig. 3, is related to the geometric parameters a , r and l . It is expected that, as for a 3D-wire grid, lower values of the metal foam apparent density correspond to lower values of the plasma frequency.

In order to prove such considerations, Equation (1) has been used to calculate the SE of a metal foam slab of thickness d . More specifically, the SE_{dB} of a slab can be obtained as the sum of three contributions. The first one is the reflection by the two interfaces (air-foam and foam-air), called return loss and commonly indicated as R . The second one is the attenuation of the transmitted wave, called absorption loss and commonly indicated as A . Finally, the third contribution is given by the multiple reflection/transmission effect, called multiple-reflection and — transmission loss and commonly indicated as M .

Consequently, SE can be evaluated as:

$$SE_{Analytical,dB} = SE_{Analytical,dB}(\omega_p, \gamma) = R_{dB} + A_{dB} + M_{dB}. \quad (2)$$

According to [12, 50], the parameters R , A , and M , are given by:

$$\begin{cases} R = \frac{(Z_0 + Z_s)^2}{4Z_0 Z_s} \\ A = \exp(ikd) \\ M = \left[1 - \frac{(Z_0 - Z_s)^2}{(Z_0 + Z_s)^2}\right] \exp(i2kd) \end{cases} \quad (3)$$

where d [m] is the thickness of the slab, k [m^{-1}] is the wave number in the medium, Z_s and Z_0 [Ω] are respectively the intrinsic impedance of the medium and the free space impedance: $k = k_0 \sqrt{\epsilon_r \mu_r} = \frac{\omega}{c_0} \sqrt{\mu_r \left(1 - \frac{\omega_p^2}{\omega^2 - j\gamma\omega}\right)}$, $Z_s = \sqrt{\frac{\mu}{\epsilon}} = \frac{Z_0}{\sqrt{1 - \frac{\omega_p^2}{\omega^2 - j\gamma\omega}}}$, $c_0 = 3 * 10^8 [\frac{m}{s}]$,

$$Z_0 = 377 \Omega.$$

It is worth underlining that, by adopting a 3D-wire mesh approximation, ω_p and γ could be evaluated as a function of the geometric parameters of the foam, as suggested and demonstrated by the same authors in [14–16]. As clarified later on, in this paper an alternative simplified approach is suggested, so as to take into account the peculiarities of the foam structure.

4. RESULTS

In this section, results related to the experimental, the numerical and the analytical evaluation of the SE of different kinds of Duocel®

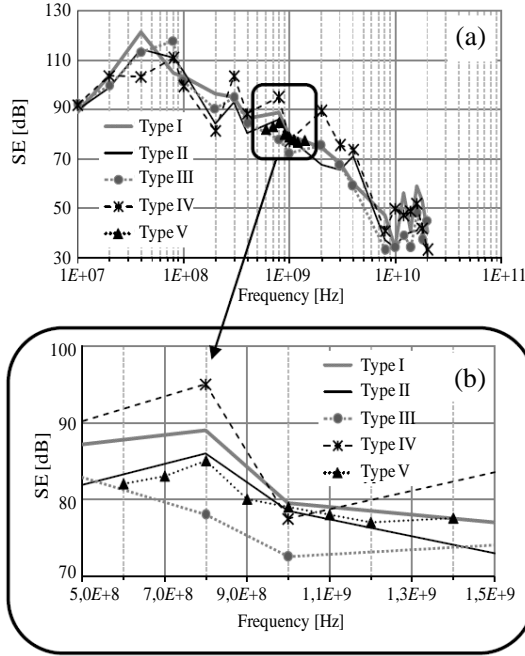


Figure 4. Shielding effectiveness (E field) for aluminum foam slabs described in Table 1. (a) Numerical results (Type V) are better highlighted in (b) the zoomed picture.

Table 1. Examined foam types.

Duocel® Aluminum foams				
Type I	Type II	Type III	Type IV	Type V (numerical model)
10 PPI, 6–8% nominal density, 6.1% actual density. Alloy 6101-F	20 PPI, 6–8% nominal density, 8.5% actual density. Alloy 6101-F	40 PPI, 6–8% nominal density, 7.9% actual density. Alloy 6101-F	40 PPI, 6–8% nominal density, 8.7% actual density. Alloy 6101-F	7 PPI, 11% actual density, numerically generated Alloy 6101-F

aluminum foam slabs are reported and discussed. In Fig. 4, for instance, the electric SE related to five open-cell slabs with a thickness of 1.4 cm is given for different structural properties (according to data summarized in Table 1). More specifically, type I-IV foams have

been considered, and measurements performed in the range 10 kHz–20 GHz; as commonly accepted, three different frequency ranges have been individuated (namely “low-frequency”, “resonance” and “high frequency”) and in each one appropriate sources have been used. The aluminum foam slabs have been carefully adapted to an aperture of a shielding room and measurements performed according to how described in the IEEE Std 299–1996 [51]. Results obtained this way, have been used to calculate the metal foams SE according to the following classical formula:

$$SE_E = 20 \log (E_1/E_2) \quad (4)$$

where E_1 and E_2 are the received electric fields evaluated respectively without and with the shield made of metal foam.

Excellent shielding capabilities, especially below 5 GHz (SE better than 70 dB), can be observed in Fig. 4. Furthermore, according to the previously hypothesized plasma behaviour of the metal foams, the SE decreases as frequency increases. Nevertheless, SE values greater than 35 dB have been obtained in the whole analyzed frequency range. More in detail, by comparing the SE values of aluminum foam slabs of type II with those of Type IV, it is noticeable that for metal foams with the same apparent density, shielding capabilities decrease as PPI increases. Moreover, when comparing slabs with the same PPI but different apparent density (Type III and Type IV), better shielding performances are observed for lower density slabs. Such results encourage a more detailed study aiming at a numerical and/or analytical evaluation of the necessary porosity and density to guarantee a desired SE.

To this aim, the implemented realistic numerical models of metal foam slabs have been used in the aforementioned parallel VM-FDTD code. In the same Fig. 4, for instance, the SE calculated by analyzing a numerical model reproducing the Type-V aluminum foam (see Table 1) is shown. The simulations have been performed in the frequency range (700 MHz–1.2 GHz); a very good agreement with experimental data can be observed.

It is worth highlighting that the numerically reproduced porosity and density do not perfectly match the actually measured samples. In fact, in order to simulate the Type-V slab, a numerical model with a discretization step of 0.5 mm has been generated through the algorithm described in Section 3.2, whereas an even smaller step would have been necessary to generate one of the experimentally measured samples. In fact, despite the VM scheme, the small time-step combined with the large simulation domain ($400 \times 600 \times 600$ cells are necessary to simulate the SE experimental set-up) implies large computing time: 24 hours have been needed to obtain only one of the reported SE values (a

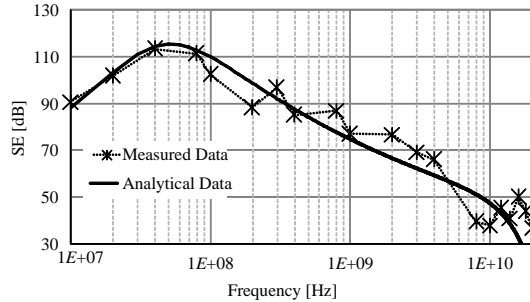


Figure 5. Shielding effectiveness (E -field) of an open-cell metal foam slab (Type III of Table 1) with a thickness of 14 mm. Comparison between measured data and analytical results obtained by solving Eqs. (2)–(3) and assuming the $f_p = 19.894$ GHz, $\gamma = 22 \times 10^7$ rad/s.

small parallel platform consisting of 12 α -Digital@667 MHz processors has been used).

Consequently, in order to overcome these shortcomings, the possibility to model metal foams as homogeneous media characterized by a Drude dispersion model has been verified by using (2)–(3) to calculate the metal foam SE. More specifically, since the analytical expression of SE is a function of ω_p and γ , such parameters have been optimized by means of a proprietary code implemented in MATLAB so to have the best fitting with measured data.

A good agreement between the analytical and the measured curves has been obtained for the following values of f_p and γ :

$$f_p = \frac{\omega_p}{2\pi} = 19.894 \text{ GHz}, \quad \gamma = 22 \times 10^7 \text{ rad/s}$$

and the corresponding results are illustrated in Fig. 5.

It emerges that, similarly to the thin wire array, aluminum-based metal foams exhibit the same behaviour of aluminum, but with a plasma frequency in the microwave range rather than in the terahertz one, confirming our previous observations. Furthermore, from comparison between numerical and analytical results, it has been verified that metal foams with a lower apparent density exhibit a lower plasma frequency.

It is worth underlining that the dispersion model given in (1) can be implemented in the VM-FDTD tool described in this paper by using one of the methods commonly adopted to introduce dispersive materials in the FDTD scheme [14, 52].

As a consequence, results reported in this section suggest the following analysis procedure for a given metal foam:

- *Step 1*: analysis of a small sample of the metal foam numerical model by using a full-wave tool, such as the VM-FDTD.
- *Step 2*: optimization of the ω_p and γ parameters which appear in (1) in order to have the best fitting between the numerical simulation results and the analytical data;
- *Step 3*: use either directly (2)–(3) for the SE estimation or implement (1) in a compatible full-wave simulator for different EM investigations.

More specifically, it can be observed that the first step is referred to the numerical analysis of a relatively small sample of metal foam. It is worth pointing out that, in this way, the analysis can be performed also through traditional computers and common full-wave EM solvers. The numerical result of this pre-processing phase is used to feed the proposed simplified analytical model, thus allowing the evaluation of optimized values of ω_p and γ parameters. In this way, differently from the approach proposed in [15], where the starting point for the evaluation of ω_p and γ is derived from the 3D-wire mesh approximation, the foam peculiarities are taken into account. Finally, once the optimization has been performed, the foam analytical model can be used to design/analyze even large EM problems involving metal foams.

5. CONCLUSION

In this work, the use of metal foams as high-added value EM shields has been addressed. Their excellent electromagnetic (EM) shielding capabilities have been verified through the Shielding Effectiveness (SE) measurement of different open-cell aluminum foam slabs. Furthermore, for design and analysis purposes, two different approaches have been proposed. The former, based on a microscopic point of view, uses a powerful EM full-wave simulator to analyze ad-hoc developed and very accurate numerical models of metal foams. Vice versa, the latter is based on a macroscopic point of view and looks at the foam as an effectively homogeneous medium. The accuracy of both numerical and analytical metal foam models has been demonstrated through comparisons with experimental data. Finally, a powerful methodology to analyze general EM problems involving metal foams has been suggested. It takes advantage from the joint use of the two presented approaches: the macroscopic parameters which electromagnetically characterize the foam are derived from a preliminary full-wave analysis of its numerical model. This way, by implementing the corresponding effectively homogeneous medium in a common full-wave simulator, SE as well as other EM analysis can be easily performed.

REFERENCES

1. Ashby, M. F., A. G. Evans, N. A. Fleck, L. J. Gibson, J. W. Hutchinson, and H. N. G. Wadley, *Metal Foams: A Design Guide*, Butterworth-Heinemann, 2000.
2. Kovacic, J., P. Tobolka, F. Simancik, J. Banhart, M. F. Ashby, and N. A. Fleck, "Metal foams and foam metal structures," *Int. Conf. Metfoam'99, MIT Verlag Bremen, Germany*, Jun. 1999.
3. Banhart, J., "Manufacture characterisation and application of cellular metals and metal foams," *Progress in Materials Science*, Vol. 46, No. 6, 559–632, 2001.
4. Deshpande, V. S. and N. A. Fleck, "Isotropic constitutive models for metallic foams," *Journal of the Mechanics and Physics of Solids*, Vol. 48, 1253–1283, 2000.
5. Hanssen, A. G., O. S. Hopperstad, M. Langseth, and H. Ilstad, "Validation of constitutive models applicable to aluminium foams," *International Journal of Mechanical Sciences*, Vol. 44, 359–406, 2002.
6. Lu, T. J. and J. M. Ong, "Characterization of close-celled cellular aluminium alloys," *Journal of Materials Science*, Vol. 36, 2773–2786, 2001.
7. Bart-Smith, H., J. W. Hutchinson, N. A. Fleck, and A. G. Evans, "Influence of imperfections on the performance of metal foam core sandwich panels," *Int. Journal of Solid and Structures*, Vol. 39, 4999–5012, 2002.
8. Youssef, S., E. Maire, and R. Gaertner, "Finite element modeling of the actual structure of cellular materials determined by X-ray tomography," *Acta Materialia*, Vol. 53, 719–730, 2005.
9. Baumeister, J., U. J. Banhart, and M. Weber, "Aluminium foams for transport industry," *Materials & Design*, Vol. 18, 217–220, 1997.
10. Han, F. S. and Z. G. Zhu, "The mechanical behavior of foamed aluminum," *Journal of Materials Science*, Vol. 34, 291–299, 1999.
11. Catarinucci, L., O. Losito, L. Tarricone, and F. Pagliara, "High added-value EM shielding by using metal-foams: Experimental and numerical characterization," *IEEE Int. Symp. on Electromagnetic Compatibility*, Vol. 2, 285–289, Aug. 2006.
12. Lovat, G. and P. Burghignoli, "Shielding effectiveness of a metamaterial slab," *IEEE Int. Symp. on Electromagnetic Compatibility*, 2007.
13. Boyvat, M. and C. Hafner, "Molding the flow of magnetic

- field with metamaterials: Magnetic field shielding,” *Progress In Electromagnetics Research*, Vol. 126, 303–316, 2012.
14. Monti, G., L. Catarinucci, and L. Tarricone, “New materials for electromagnetic shielding: Metal foams with plasma properties,” *Microwave and Optical Technology Letters*, Vol. 52, No. 8, 1700–1705, Aug. 2010.
 15. Monti, G., L. Catarinucci, and L. Tarricone, “Metal foams for electromagnetic shielding: A plasma model,” *Proc. of European Conference on Antennas and Propagation, EuCAP 2009*, 2123–2126, 2009.
 16. Monti, G., L. Catarinucci, and L. Tarricone, “Experimental validation of a plasma model for electromagnetic metal foam shields,” *IEEE MTT-S International Microwave Symposium Digest*, 145–148, 2009.
 17. Catarinucci, L., P. Palazzari, and L. Tarricone, “A parallel variable-mesh FDTD tool for the solution of large electromagnetic problems,” *Proc. of 19th IEEE International Parallel and Distributed Processing Symposium, IPDPS 2005*, Denver, CO, 2005.
 18. Catarinucci, L., P. Palazzari, and L. Tarricone, “Parallel FDTD simulation of radiobase antennae,” *Radiation Protection Dosimetry*, Vol. 97, No. 4, 409–413, 2001.
 19. Catarinucci, L., P. Palazzari, and L. Tarricone, “A parallel FDTD tool for the solution of large dosimetric problems: An application to the interaction between humans and radiobase antennas,” *IEEE MTT-S International Microwave Symposium Digest*, Vol. 3, 1755–1758, 2002.
 20. Catarinucci, L., P. Palazzari, and L. Tarricone, “Human exposure to the near field of radiobase antennas — A full-wave solution using parallel FDTD,” *IEEE Transactions on Microwave Theory and Techniques*, Vol. 51, No. 3, 935–940, 2003.
 21. De Donno, D., A. Esposito, L. Tarricone, and L. Catarinucci, “Introduction to GPU computing and CUDA programming: A case study on FDTD,” *IEEE Antennas and Propagation Magazine*, Vol. 52, No. 3, 116–122, 2010.
 22. Catarinucci, L., P. Palazzari, and L. Tarricone, “On the use of numerical phantoms in the study of the human-antenna interaction problem,” *IEEE Antennas and Wireless Propagation Letters*, Vol. 2, 43–45, 2003.
 23. Catarinucci, L. and L. Tarricone, “A parallel graded-mesh FDTD algorithm for human-antenna interaction problems,” *International Journal of Occupational Safety and Ergonomics*, Vol. 15, No. 1,

- 45–52, 2009.
24. Taflove, A., *Computational Electrodynamics: The Finite Difference Time-domain Method*, Artech House, Norwood, MA, 1995.
 25. Shelby, R. A., D. R. Smith, S. C. Nemat-Nasser, and S. Schultz, “Microwave transmission through a two-dimensional, isotropic, left-handed metamaterial,” *Appl. Phys. Lett.*, Vol. 78, No. 4, 489–491, Jan. 2001.
 26. Vendik, I., O. Vendik, I. Kolmakov, and M. Odit, “Modelling of isotropic double negative media for microwave applications,” *Opto-Electronics Review*, Vol. 14, No. 3, 179–186, 2006.
 27. Monti, G. and L. Tarricone, “Negative group velocity in a split ring resonator-coupled microstrip line,” *Progress In Electromagnetics Research*, Vol. 94, 33–47, 2009.
 28. Monti, G. and L. Tarricone, “Signal reshaping in a transmission line with negative group velocity behaviour,” *Microwave Optical Technology Letters*, Vol. 51, No. 11, 2627–2633, 2009.
 29. Monti, G. and L. Tarricone, “Dispersion analysis of a planar negative group velocity transmission line,” *Proceedings of the 37th European Microwave Conference, EUMC*, 1644–1647, 2007.
 30. Monti, G. and L. Tarricone, “Compact broadband monolithic 3-dB coupler by using artificial transmission lines,” *Microwave and Optical Technology Letters*, Vol. 50, No. 10, 2662–2667, 2008.
 31. Monti, G. and L. Tarricone, “Reduced-size broadband CRLH-ATL rat-race coupler,” *Proceedings of the 36th European Microwave Conference, EuMC 2006*, 125–128, 2007.
 32. Wang, C.-W., T.-G. Ma, and C.-F. Yang, “A new planar artificial transmission line and its applications to a miniaturized butler matrix,” *IEEE Transactions on Microwave Theory and Techniques*, Vol. 55, No. 12, 2792–2801, 2007.
 33. Monti, G. and L. Tarricone, “Dual-band artificial transmission lines branch-line coupler,” *International Journal of RF and Microwave Computer-Aided Engineering*, Vol. 18, No. 1, 53–62, 2008.
 34. Monti, G., R. de Paolis, and L. Tarricone, “Design of a 3-state reconfigurable CRLH transmission line based on MEMS switches,” *Progress In Electromagnetics Research*, Vol. 95, 283–297, 2009.
 35. Eccleston, K. W. and S. H. M. Ong, “Compact planar microstrip line branch-line and rat race coupler couplers,” *IEEE Transactions on Microwave Theory and Techniques*, Vol. 51, No. 10, 2119–2125, Oct. 2003.
 36. Monti, G. and L. Tarricone, “A novel theoretical formulation for

- the analysis of the propagation of finite-bandwidth signals in a double-negative slab,” *Microwave and Optical Technology Letters*, Vol. 47, No. 5, 434–439, 2005.
37. Monti, G. and L. Tarricone, “Gaussian pulse expansion of modulated signals in double-negative slab,” *IEEE Transactions on Microwave Theory and Techniques*, Vol. 54, No. 6, 2755–2761, 2006.
 38. Choy, T. C., *Effective Medium Theory: Principles and Applications* Clarendon, Oxford University Press, New York, 1999.
 39. Monti, G. and L. Tarricone, “Dispersion analysis of an negative group velocity medium with MATLAB,” *Applied Computational Electromagnetics Society Journal*, Vol. 24, No. 5, 478–486, Oct. 2009.
 40. Monti, G. and L. Tarricone, “On the propagation of a Gaussian pulse in a double-negative slab,” *Proc. 35th European Microwave Conference*, 1419–1422, 2005.
 41. Drude, P., *Ann. Phys.*, Vol. 1, 566, Leipzig, 1900.
 42. Ashcroft, N. W. and N. D. Mermin, *Solid State Physics*, Saunders Co., Philadelphia, 1976.
 43. Pendry, J. B., A. J. Holden, D. J. Robbins, and W. J. Stewart, “Low frequency plasmons in thin-wire structures,” *J. Phys.: Condens. Matter*, Vol. 10, 4785–4809, 1998.
 44. Silveirinha, M. G. and C. A. Fernandes, “Homogenization of 3-D-connected and nonconnected wire metamaterials,” *IEEE Trans. on Microw. Theory and Techniques*, Vol. 53, No. 4, Apr. 2005.
 45. Maslovski, S. I., S. A. Tretyakov, and P. A. Belov, “Wire media with negative effective permittivity: A quasi static model,” *Microwave Optical Technology Letters*, Vol. 35, No. 1, 47–51, Oct. 2002.
 46. Tretyakov, S., *Analytical Modeling in Applied Electromagnetics*, Artech House, Norwood, MA, 2003.
 47. Lee, J.-Y., J.-H. Lee, H.-S. Kim, N.-W. Kang, and H.-K. Jung, “Effective medium approach of left-handed material using a dispersive FDTD method,” *IEEE Trans. on Magnetic*, Vol. 41, No. 5, 1484–1487, May 2005.
 48. Moses, C. A. and N. Engheta, “Electromagnetic wave propagation in the wire medium: A complex medium with long thin inclusions,” *Wave Motion*, Vol. 34, No. 3, 239–352, 2001.
 49. Pendry, J. B., A. J. Holden, D. J. Robbins, and W. J. Stewart, “Low frequency plasmons in thin-wire structures,” *J. Phys.: Condens. Matter*, Vol. 10, 4785–4809, 1998.

50. Paul, C. R., *Introduction to Electromagnetic Compatibility*, Wiley, 1992.
51. “IEEE Standard method for measuring the effectiveness of electromagnetic shielding enclosures,” IEEE Std 299–2006, Feb. 2007.
52. Catarinucci, L., G. Monti, and L. Tarricone, “A parallel-grid-enabled variable-mesh FDTD approach for the analysis of slabs of double-negative metamaterials,” *IEEE Antennas and Propagation Society, AP-S International Symposium (Digest)*, Vol. 3A, 782–785, Washington, Jul. 2005.